

Input characteristics of a non-ideal DC-DC flyback converter

W. JANKE, M. BĄCZEK, and J. KRAŚNIEWSKI*

Department of Electronics and Computer Science, Koszalin University of Technology, 2 Śniadeckich St., 75-453 Koszalin, Poland

Abstract. AC and DC input characteristics of the flyback converter are analysed and investigated via Spice simulations and measurements. The influence of parasitic effects in converter components on input characteristics is studied in continuous conduction mode (CCM) and discontinuous conduction mode (DCM). The results of the calculations based on analytical formulas and averaged models are in a good accordance with Spice simulations and measurements.

Key words: flyback, DC-DC converter, input characteristics, parasitic effects.

1. Introduction

Flyback DC-DC switch-mode converter is a very popular power with many applications because of its unique features such as the galvanic isolation between input and output, the wide range of possible voltage transfer function and the possibility to supply many isolated loads. The elementary descriptions of flyback converters can be found in textbooks, as for example [1–3], and many aspects of their properties, applications and control methods are presented in many sources, for example in [4–13]. There is a difference between the non-ideal description of a converter in which the parasitic effects (parasitic capacitances, series resistances and inductances of components etc.) are included and the ideal description, where they are not. The input characteristics of a non-ideal flyback are not presented in the systematic way in the literature, although they may be important in some applications of flyback, for example in power factor correction (PFC) or maximum power point tracing (MPPT) circuits. The aim of this paper is the investigation of the input characteristics of flyback working in continuous conduction mode (CCM) and discontinuous conduction mode (DCM) by analysis, simulation and measurements. A special attention is paid to the influence of parasitic effects in the converter on its input characteristics.

The basic scheme of the power stage of flyback converter including a transformer with the winding ratio $n = N_{sec}/N_{prim}$, is shown in Fig. 1. The waveforms of currents and voltages in a power stage of switch-mode DC-DC converter are very complex because of the switching nature of a converter action. In particular, parasitic oscillations resulting from switching processes are observed. These oscillations may be only partially suppressed by so called snubbers. The exemplary waveforms of the input current measured for flyback in the short time scale (several switching periods) are shown in Fig. 2, where the continuous and discon-

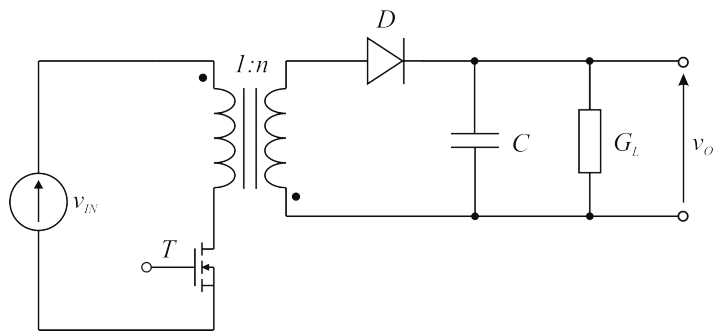


Fig. 1. The power stage of a flyback converter

tinuous conduction modes are distinguished and the influence of the eventual use of snubber is seen. Input voltage: $V_G = 24$ V, switching frequency: $f_S = 100$ kHz, duty ratio: $D_A = 0.5$; primary winding inductance: $L = 170$ μ H, turns ratio: $n = 0.2$, output capacitance: $C = 470$ μ F, load resistance: 3 Ω for a) and b), 50 Ω for c) and d). A simple snubber formed by a diode, resistor and capacitor is connected at the input terminals of the transformer.

External features of a switching converter for steady state or slow transients are usually described by the dependencies between currents and voltages averaged over a single switching period, in other words, by averaged models [1–5, 7]. In a typical description of DC-DC switching converters, the small-signal averaged input-to-output voltage transfer function and control-to-output transmittance are used and the formulas describing these characteristics may be found in many sources. The averaged descriptions of flyback converters presented in the literature usually concern the idealized converter models in which the parasitic effects are not included or included only partially [1–3, 6–12]. The mentions concerning the averaged input characteristics of ideal flyback can be found in [1] and [7]. Averaged models of a non-ideal flyback are considered to the limited extent in the literature, and the most representative example seems to be the paper [13] in which the modifications of the standard state-space averaging and the switch averaging

*e-mail: jaroslaw.krasniewski@ie.tu.koszalin.pl

Manuscript submitted 2019-03-04, revised 2019-06-17, initially accepted for publication 2019-07-10, published in October 2019

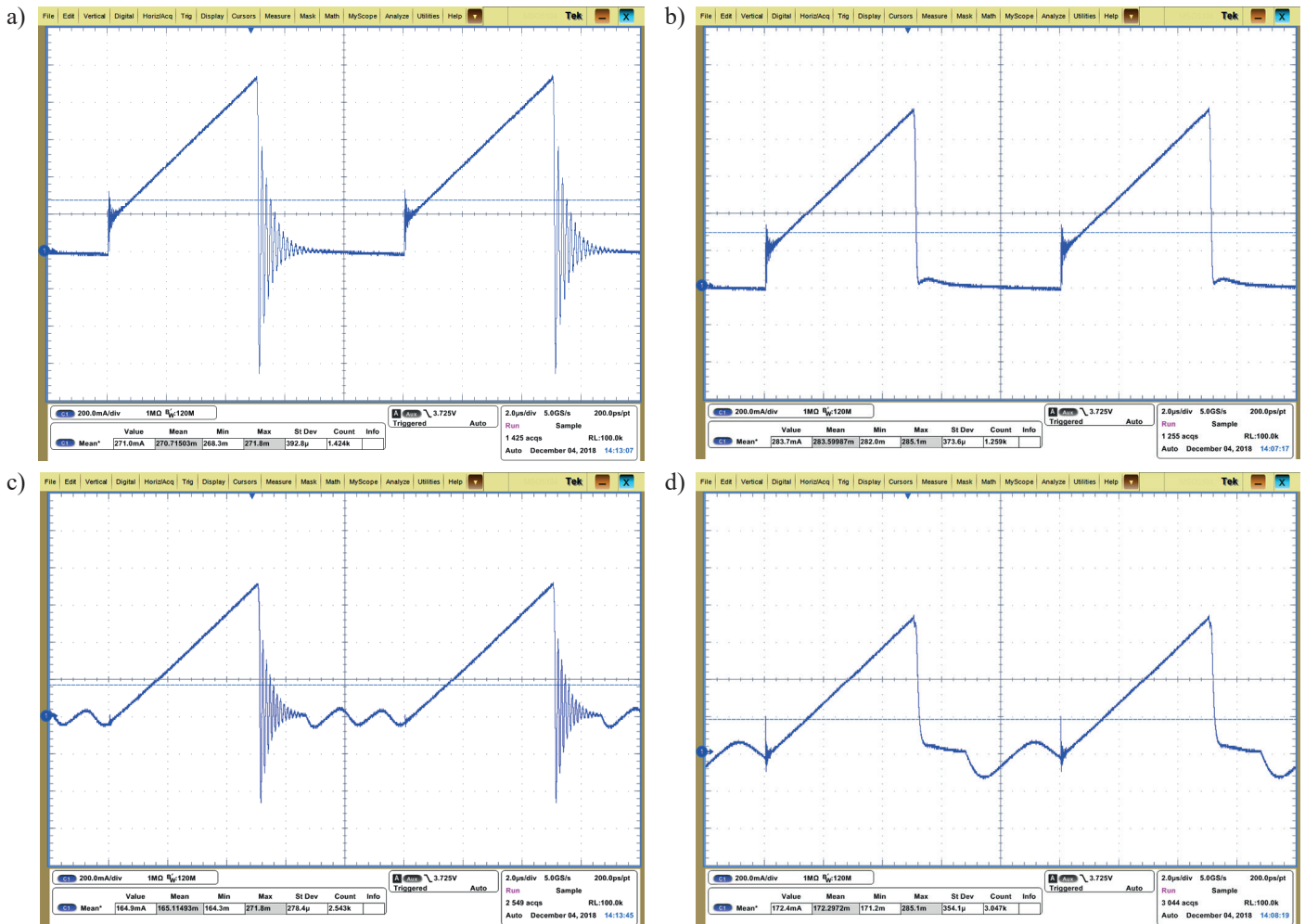


Fig. 2. Waveforms of the input current of flyback: a) CCM without snubber, b) CCM with snubber, c) DCM without snubber, d) DCM with snubber

technique, specific for a flyback converter, are introduced, with the parasitic resistances of all converter components included, but the input characteristics of a non-ideal flyback is not considered. Flybacks used in AC-DC converters are working in DCM or BCM (boundary between CCM and DCM) more frequently than in CCM [14–18]. It is caused by the differences in the input characteristics in CCM and DCM but this problem is not explained precisely in [14–18].

The DC input characteristics of an ideal flyback converter and the converter with the parasitic resistances of components are discussed in Sections 2 and 3. The input dynamic characteristics measured and simulated with inertial parasitic effects included, are presented in Section 4. Some concluding remarks are given in Section 5.

2. A simplified descriptions of an ideal flyback converter for direct currents (DC)

The known, basic description of the ideal flyback circuit without parasitic components [1–3] is briefly reviewed in this section. The description of the basic characteristics of the converter

working in CCM differs from the description for DCM. The boundary between CCM and DCM mode for steady state conditions may be characterized by the threshold value of the load conductance G_C , given for an ideal converter in [3].

The DC voltage transfer function M_V for ideal flyback working in continuous conduction mode (CCM) and in discontinuous conduction mode (DCM) are given by simple, known formulas [1–3].

In an ideal flyback working in CCM, similarly as in such converters as buck and boost, the voltage transfer function M_V is independent of the load. The eventual dependence of M_V on G_L may be caused by the second-order parasitic effects. The DC input conductance G_{IN} of an ideal loss-less converter may be easily found from the condition of the equality of the input and output DC power, and is proportional to the load conductance G_L [1, 2]:

$$G_{INi} = \frac{I_{IN}}{V_{IN}} = M_{Vi}^2 \cdot G_L. \quad (1)$$

The formulas for the input conductance of the ideal flyback in CCM and DCM respectively are:

$$G_{INi}(CCM) = \frac{n^2 \cdot D_A^2}{(1 - D_A)^2} \cdot G_L$$

$$G_{INi}(DCM) = \frac{T_S}{2 \cdot L} \cdot D_A^2$$

where T_S is switching period.

The basic difference between the above formulas concerns the dependence of the input conductance on the load conductance.

The expression for the input characteristics of the ideal flyback in DCM may be deduced from chapters 11 and 18 of textbook [1] by Erickson and Maksimovic. In Ch. 11, based on earlier works of the same authors, the concept of so called “loss-free resistor” R_e is introduced as a component of the averaged model of the pair of ideal switches in buck, boost and buck-boost converters working in DCM (the second component is a controlled power source). The expression for the resistance of “loss-free resistor” is [1]:

$$R_e = \frac{2 \cdot L}{D_A^2 \cdot T_S} \tag{4}$$

From the discussion in Ch. 18 of [1], it may be inferred that the input resistance of ideal flyback in DCM is equal to the resistance of this “loss-free resistor”. The models of converters working in DCM, containing loss-free resistor and controlled power source presented in [1] are not accepted by circuit simulators, e.g. Spice, therefore the usefulness of such models is limited, nevertheless the conductance obtained as the reciprocal of (4) is precisely equal to (3).

The averaged large-signal and small-signal description of an ideal flyback in CCM as well as in DCM is systematically presented in [7]. It is worth noting, that the input characteristics of flyback in DCM given in [7] differ qualitatively from characteristics resulting from the description in [1]. The differences between some characteristics for DCM obtained in [7] and in the present paper are discussed in further sections.

3. Input characteristics of a non-ideal flyback converter for direct currents

The DC input current of a non-ideal flyback converter may be calculated as the averaged value of the time-dependence of the instantaneous input current $i_{IN}(t)$ over a single switching period. The equivalent circuit used in this section for finding the relations between currents and voltages averaged over switching period for steady state is depicted Fig. 3, where the transformer is replaced by two controlled sources and magnetizing inductance L (the inductance of the primary winding), and semiconductor switches are represented by symbols S_1 and S_2 .

Resistances R_1 and R_2 include parasitic resistances of switches and of primary and secondary windings of the transformer. The inertial parasitic effects such as capacitances of

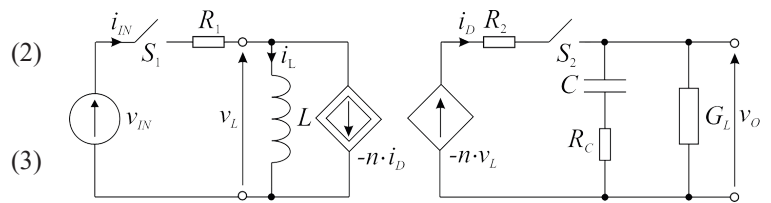


Fig. 3. The equivalent circuit of the flyback power stage

semiconductor switches and leakage inductances of transformer are not included in Fig. 3 and in the analytical description presented in this section.

The switching period T_S contains two or three sub-intervals with different states of switches. For DCM there are three sub-intervals: ON (S_1 ON, S_2 OFF), OFF1 (S_1 OFF, S_2 ON) and OFF2 (both switches OFF) and the equivalent circuits of the converter are depicted in Fig. 4a, b and c respectively. The situation for the CCM mode is simpler, because the OFF2 sub-interval doesn't exist.

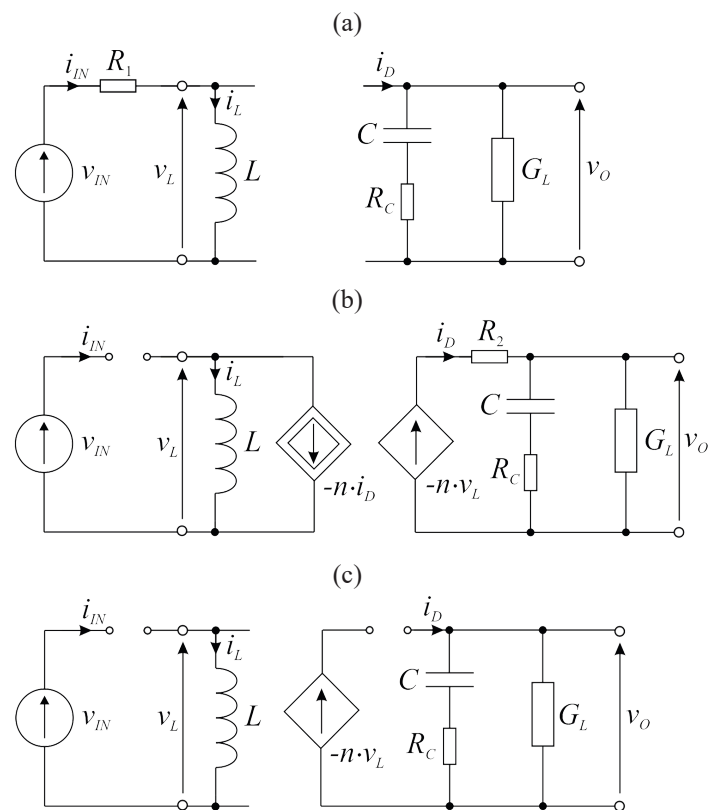


Fig. 4. Equivalent circuits of flyback in three sub-intervals: a) ON, b) OFF1, c) OFF2

The steady state conditions are considered in this section (input voltage V_{IN} , load conductance G_L and duty ratio D_A of switching signal are constant). The input current waveform $i_{IN}(t)$ of the converter in the single switching period, according to Fig. 4 is:

$$i_{IN}(t) = \begin{cases} i_L(t) & \text{for } 0 \leq t < t_{ON} \\ 0, & \text{for } t_{ON} \leq t < T_S \end{cases} \quad (5)$$

where: $t_{ON} = D_A \cdot T_S$. For convenience, the considered switching period begins at $t = 0$.

The input current averaged over single switching period is:

$$\langle i_{IN}(t) \rangle = \frac{1}{T_S} \cdot \int_0^{T_S} i_{IN}(t) \cdot dt = \frac{1}{T_S} \cdot \int_0^{t_{ON}} i_L(t) \cdot dt \quad (6)$$

and is equal to the DC term I_{IN} of the input current:

$$\langle i_{IN}(t) \rangle = I_{IN}. \quad (7)$$

The waveform of the $i_L(t)$ for $0 \leq t \leq t_{ON}$, obtained from the equation:

$$V_{IN} = i_L \cdot R_1 + L \cdot \frac{di_L}{dt} \quad (8)$$

(see Fig. 4a), is:

$$i_L(t) = \frac{V_{IN}}{R_1} \cdot \left[1 - e^{\left(-\frac{R_1}{L} \cdot t\right)} \right] + i_L(0) \cdot e^{\left(-\frac{R_1}{L} \cdot t\right)}. \quad (9)$$

By substitution of (9) into (6) one obtains:

$$I_{IN} = \frac{V_{IN}}{R_1 \cdot T_S} \cdot \left\{ t_{ON} + \frac{L}{V_{IN}} \cdot \left[i_L(0) - \frac{V_{IN}}{R_1} \right] \left[1 - e^{\left(-\frac{R_1}{L} \cdot t_{ON}\right)} \right] \right\}. \quad (10)$$

In the special case of DCM mode we have $i_L(0) = 0$ and the simplified form of Eqn. (10) is obtained:

$$I_{IN}(DCM) \cong \frac{V_{IN}}{R_1 \cdot T_S} \cdot \left\{ t_{ON} + \frac{L}{R_1} \left[e^{\left(-\frac{R_1}{L} \cdot t_{ON}\right)} - 1 \right] \right\}. \quad (11)$$

Note, that in Eqns. (9–11), for $R_1 = 0$, undefined symbols $0/0$ or $0 \cdot \infty$ are obtained. The case of $R_1 \rightarrow 0$ is considered below. Using in Eqn. (14) the approximation:

$$e^{-x} = 1 - x + \frac{x^2}{2} \text{ for } x \ll 1 \quad (12)$$

with

$$x = \frac{R_1}{L} \cdot t_{ON} \quad (13)$$

we obtain:

$$I_{IN} \cong i_L(0) \cdot D_A \cdot (1 - R_1 \cdot D_A \cdot G_Z) + V_{IN} \cdot D_A^2 \cdot G_Z \quad (14)$$

where:

$$G_Z = \frac{T_S}{2 \cdot L} \quad (15)$$

and t_{ON} is replaced by $D_A \cdot T_S$.

It may be easily proved, that the expression (12), with x given by (13) is a very good approximation for Eqn. (9) and real values of converter parameters assumed. Taking exemplary values: $R_1 = 0.55 \Omega$, $L = 170 \mu\text{H}$, $D_A = 0.4$, $T_S = 10 \mu\text{s}$ (corresponding to laboratory model of flyback used in experiments described below), one obtains: $x = 0.0129$ therefore the first omitted term in expansion (12) is nearly seven orders of magnitude smaller than the exact value of e^{-x} .

Further calculations for CCM and DCM are different. In DCM the initial value of current, $i_L(0)$ is simply zero and the averaged input current is:

$$I_{IN} \cong \frac{V_{IN}}{2 \cdot L} \cdot D_A^2 \cdot T_S \quad (16)$$

and the input conductance of flyback in DCM is:

$$G_{IN}(DCM) = \frac{I_{IN}}{V_{IN}} \cong G_Z \cdot D_A^2 \quad (17)$$

in accordance with Eqn. (3).

It should be pointed out, that the simple form of the expression (17) is not the result of the ideality of the converter assumed a priori but is obtained as a very good numerical approximation (12) in the equation (10). The formula for DC input current of an ideal flyback in DCM presented in [7] is different, namely:

$$I_{IN} = \frac{V_{IN}}{2 \cdot L} \cdot D_A^2 \cdot T_S + n \cdot G_L \cdot V_O \quad (18)$$

and may be expressed as:

$$I_{IN} = D_A^2 \cdot G_Z \cdot V_{IN} + n \cdot D_A \cdot V_{IN} \cdot \sqrt{G_Z \cdot G_L}. \quad (19)$$

The additional term in Eqns. (18) and (19), proportional to the square root of the load conductance, is the result of introducing the “correction factor” in [6] proposed for DCM in [19].

For CCM mode, the quantity $i_L(0)$ in (10) should be found. It may be achieved starting with approximation of Eqn. (9) based on the approximate expansion $e^{-x} \cong 1 - x$:

$$i_L(t) \cong i_L(0) + [V_{IN} - R_1 \cdot i_L(0)] \cdot t / L. \quad (20)$$

The maximum value i_{LM} of $i_L(t)$ is:

$$i_{LM} \cong i_L(0) + [V_{IN} - R_1 \cdot i_L(0)] \cdot t_{ON} / L. \quad (21)$$

The averaged value I_L of $i_L(t)$ is:

$$I_L \cong i_L(0) + \frac{i_{LM} - i_L(0)}{2} = i_L(0) + [V_{IN} - R_1 \cdot i_L(0)] \cdot D_A \cdot G_Z. \quad (22)$$

From Eqn. (22) one obtains:

$$i_L(0) \cong \frac{I_L - V_{IN} \cdot D_A \cdot G_Z}{1 - R_1 \cdot D_A \cdot G_Z}. \quad (23)$$

Introducing (23) into (14), after simple manipulations, one obtains:

$$I_{IN} \cong D_A \cdot I_L. \quad (24)$$

The DC value of current $i_L(t)$ may be expressed as [20]:

$$I_L = \frac{n}{1 - D_A} \cdot G_L \cdot M_V \cdot V_{IN}. \quad (25)$$

The DC voltage transfer function M_V of non-ideal flyback in CCM is described in [20] as:

$$M_V = \frac{M_{Vi}}{1 + G_L \cdot R_{EQ} \cdot \frac{n^2}{(1 - D_A)^2}} \quad (26)$$

where M_{Vi} is the value of M_V for an ideal case and the equivalent parasitic resistance is:

$$R_{EQ} = D_A \cdot R_1 + (1 - D_A) \cdot \frac{R_2}{n^2}. \quad (27)$$

From Eqns. (24), (25) and (26):

$$I_{IN}(CCM) = \frac{G_L \cdot M_{Vi}^2 \cdot V_{IN}}{1 + G_L \cdot R_{EQ} \cdot \frac{n^2}{(1 - D_A)^2}} \quad (28)$$

and

$$G_{IN}(CCM) = \frac{G_L \cdot M_{Vi}^2}{1 + G_L \cdot R_{EQ} \cdot \frac{n^2}{(1 - D_A)^2}}. \quad (29)$$

In the most frequently used step-down flyback, $n^2 \ll 1$ and the expression for the equivalent resistance may be approximated as:

$$R_{EQ} \cong (1 - D_A) \cdot \frac{R_2}{n^2} \quad (30)$$

and, consequently

$$G_{IN}(CCM) \cong \frac{G_L \cdot M_{Vi}^2}{1 + G_L \cdot \frac{R_2}{(1 - D_A)}}. \quad (31)$$

The DC input characteristics of flyback have been observed by measurements and numerical simulations. The laboratory model of the power stage of flyback used in experiments has the same data as mentioned in the Introduction. Other parameters for particular measurements and simulations are different.

Simulations are performed in the Mathcad software with the use of equations presented in this section in two variants – with parasitic resistances included or omitted. Another group of calculations is performed in Spice simulator (full-wave simulations with numerically finding the averaged value of the input current $i_{IN}(t)$ for each switching cycle). The diode is represented by the model corresponding to MBRD1035 in Spice library and the transistor is described by library models of MOSFET (IRFZ44) or HEMT (TPH3206). The parasitic resistances and inductances of primary ($R_{L1} = 0.5 \Omega$, $L_{RP} = 1 \mu\text{H}$) and secondary ($R_{L2} = 23 \text{ m}\Omega$, $L_{RS} = 10 \text{ nH}$) windings and equivalent series resistance of capacitor $R_C = 72 \text{ m}\Omega$ are included. The curves shown in Figs. 5–7 correspond to converter working in CCM or DCM, where the boundary values of the load conductance, for duty ratio D_A equal to 0.2; 0.3; 0.4 or 0.5 are $G_C = 0.47$; 0.36; 0.26 or 0.18 [S] respectively.

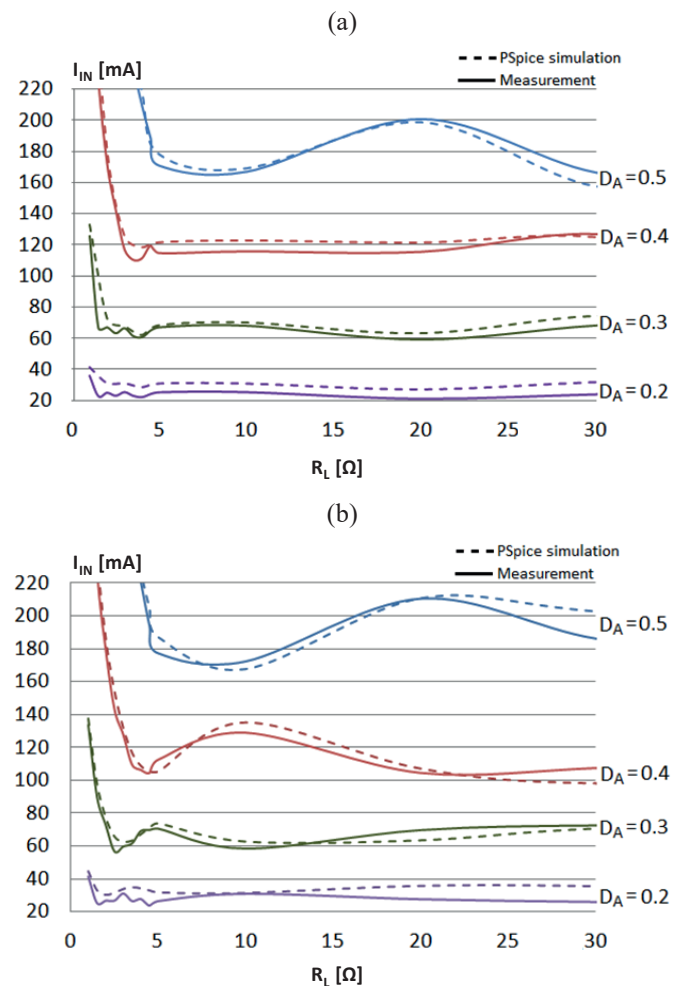


Fig. 5. Input current I_{IN} as a function of load resistance R_L : a) without snubber; b) with simple RC snubber [21] $R = 100 \Omega$, $C = 0.99 \text{ nF}$

The dependencies of the input current I_{IN} on the load resistance R_L for constant input voltage $V_{IN} = 24 \text{ V}$ and different duty ratio shown in Fig. 5 are obtained by measurements or Spice simulations (with HEMT used as the main switch). Lower

values of R_L correspond to CCM and higher – to DCM. The calculations of I_{IN} for DCM, from Eqn. (16) for $D_A = 0.3$; 0.4 and 0.5 give the values 0.064; 0.113 and 0.176 A respectively, being in relatively good accordance with measurements and PSpice simulations. The changes of I_{IN} with R_L observed by simulations and measurements are the result of parasitic oscillations corresponding to switching (see Fig. 2).

The comparison of the calculations based on equations presented in this section with full-wave Spice simulations for constant duty ratio $D_A = 0.5$ are presented in Figs. 6 and 7. The DC input characteristics $I_{IN} = f(V_{IN})$ for different values of the load resistance, shown in Fig. 6 are obtained analytically (equations 19 and 28) or by Spice simulations with different library models of the switch.

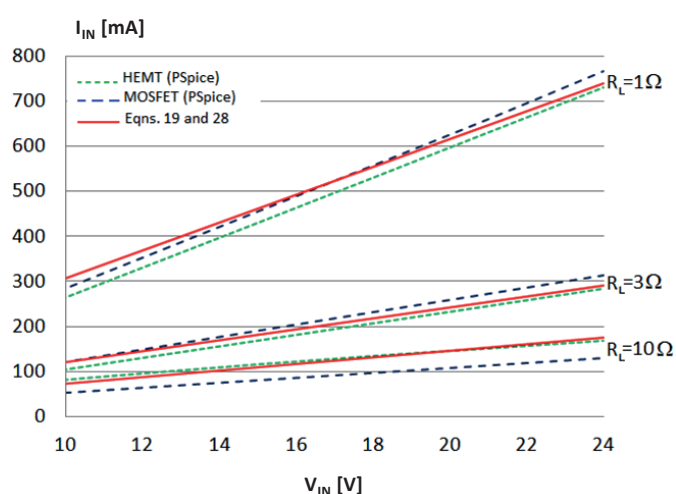


Fig. 6. Calculations of DC input characteristics $I_{IN} = f(V_{IN})$ for different load resistances R_L

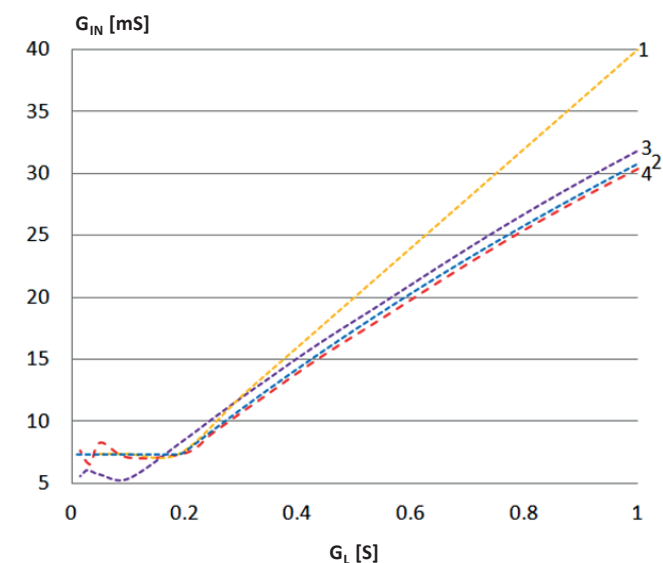


Fig. 7. The dependence of DC input conductance G_{IN} on load conductance G_L : 1 – calculations on Equations (2 and 3), 2 – calculations on Equations (17 and 29), 3 – full-wave simulation (MOSFET), 4 – full-wave simulation (HEMT)

The dependencies of the DC input conductance G_{IN} on the load conductance G_L for $V_{IN} = 24$ V, shown in Fig. 7, are calculated from the idealized formulas 2 and 3 (curve 1) or from non-ideal equations (17 and 29), or by Spice simulations with two variants of the switch model.

4. AC input characteristics

The dynamic (or AC) input characteristics of converter may be presented in the form of the time-domain response of the input current to the step change of the input voltage or in s -domain in the form of a small-signal input admittance Y_{in} . Fast transients of the input current inside a single switching period have been presented in Fig. 2. The slow transients representing the changes of input current on the longer time scale (many switching periods) better represent the effective external behavior of the converter. Slow input transients in flyback may be observed experimentally or calculated with the use of averaged dynamic models presented in [20]; may be also obtained with accurate simulations on the full-waveforms. The input cell of averaged models of flyback, shown in Fig. 8 has the same form for CCM and DCM, but the descriptions of the current source $i_{IN}(t)$ are different [20].

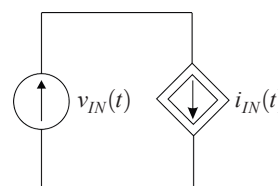


Fig. 8. The input cell of averaged models of flyback

For DCM, the current $i_{IN}(t)$ is described identically as its DC term:

$$i_{IN}(t) \cong G_Z \cdot D_A^2 \cdot v_{IN}(t) \tag{32}$$

Input current for CCM in averaged model [20] is described as:

$$i_{IN}(t) \cong D_A \cdot i_L(t) \tag{33}$$

and the current $i_L(t)$ for constant duty ratio D_A and given $v_{IN}(t)$ may be obtained by the simulation of sub-circuit shown in Fig. 9, where:

$$\gamma = \frac{1 - D_A}{n} \tag{34}$$

The observations of the slow input transients in flyback converter have been performed for the same laboratory model of converter as described in Sec. 3. Figures 10 and 11 show the response of the input current $i_{IN}(t)$ on the step change of the input voltage for CCM and DCM. Curves 1, 2 and 3 represent

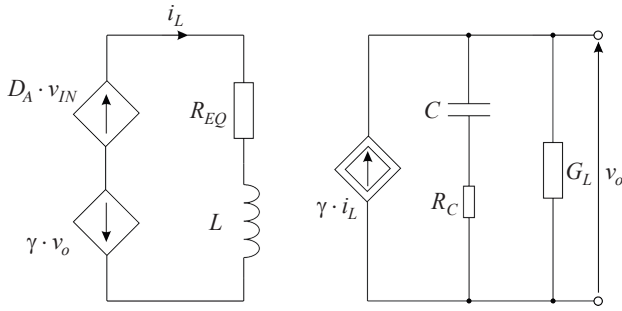


Fig. 9. Sub-circuit of the averaged model from [20]

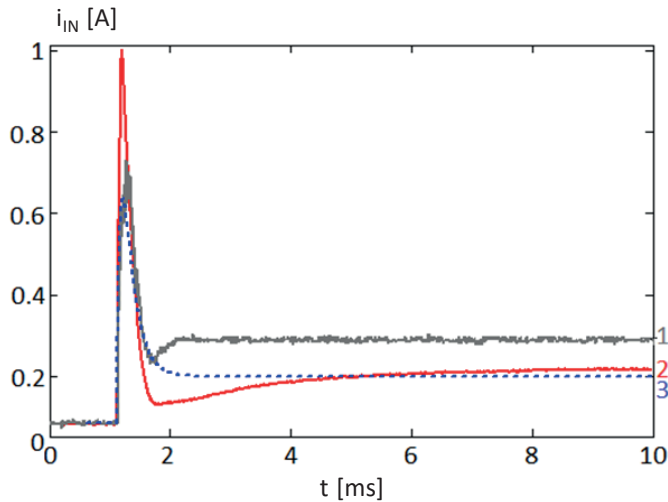


Fig. 10. The input current response to the input voltage step from 10 to 20 V in CCM: 1 – full-wave simulation, 2 – measurement, 3 – simulation based on the averaged model

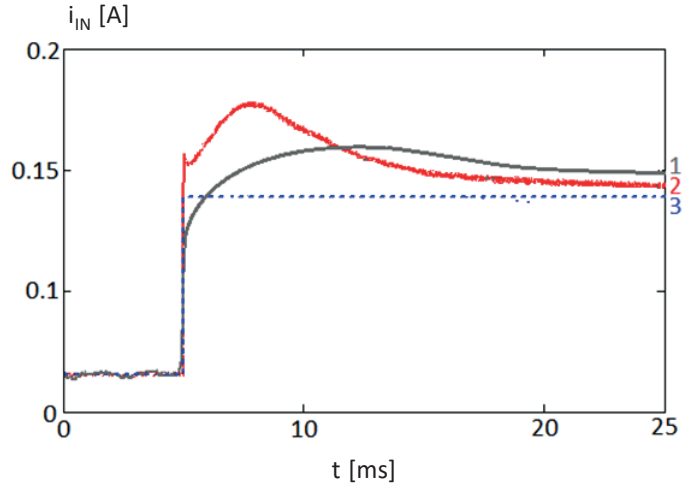


Fig. 11. The input current response to the input voltage step from 10 to 20 V in DCM: 1- full-wave simulation, 2 – measurement, 3 – simulation based on the average model

the results of simulations with the use of averaged models, full-wave simulations and measurements respectively.

The s -domain input admittance of converter is obtained from the model being the small-signal equivalent of the large-signal model. The admittance Y_{in} for DCM, in accordance with Eqn. (32) is simply equal to DC input conductance:

$$Y_{in}(DCM) = G_{IN}(DCM) \cong G_Z \cdot D_A^2. \quad (35)$$

The input admittance for CCM, derived from the large signal model presented in Figs. 8 and 9 may be expressed as:

$$Y_{in}(CCM) = \frac{D_A \cdot (s \cdot C_{EQ} + G_L)}{s^2 \cdot L \cdot C_{EQ} + s \cdot (G_L \cdot L + R_{EQ} \cdot C_{EQ} + \gamma^2 \cdot C \cdot R_C) + R_{EQ} \cdot G_L + \gamma^2} \quad (36)$$

where:

$$C_{EQ} = C \cdot (1 + G_L \cdot R_C), \quad (37)$$

The frequency dependencies of the magnitude and phase of the input admittance of flyback for DCM and CCM calculated from analytical dependencies (35) and (36) or obtained by the full-wave Spice simulation for the exemplary set of converter parameters are presented in Figs. 12 and 13. The parameters are nearly the same as mentioned in Introduction, with the exception of duty ratio for DCM, equal $D_A = 0.3$.

There is a substantial difference between the frequency dependencies of the input admittance of a flyback for CCM and DCM, obtained analytically as well as by full-wave Spice simulations. The magnitude and phase of the input admittance of flyback in DCM in the low-frequency range are nearly independent of frequency.

According to the averaged models of flyback presented by Vu in [7], the description of the small-signal admittance in CCM

is similar to equation (36) (without the parasitic resistances). The formula presented in [7] for input admittance for DCM differs substantially from (35) and has the form:

$$Y_{in}(DCM, Vu) = \frac{s \cdot \frac{D_A \cdot (M+2)}{L} + \frac{2D_A \cdot (M+1)}{R_L \cdot L \cdot C}}{s^2 + s \cdot \left(\frac{2M}{D_A \cdot T_S} + \frac{1}{R_L \cdot C} \right) + \frac{4M}{D_A \cdot T_S \cdot R_L \cdot C}} \quad (38)$$

where “the correction factor” is described as:

$$M = \frac{D_A}{n} \cdot \sqrt{R_L \cdot G_Z}. \quad (39)$$

The description of the input admittance expressed by (38) has a single zero and two real poles and does not agree with our results of the full-wave simulations.

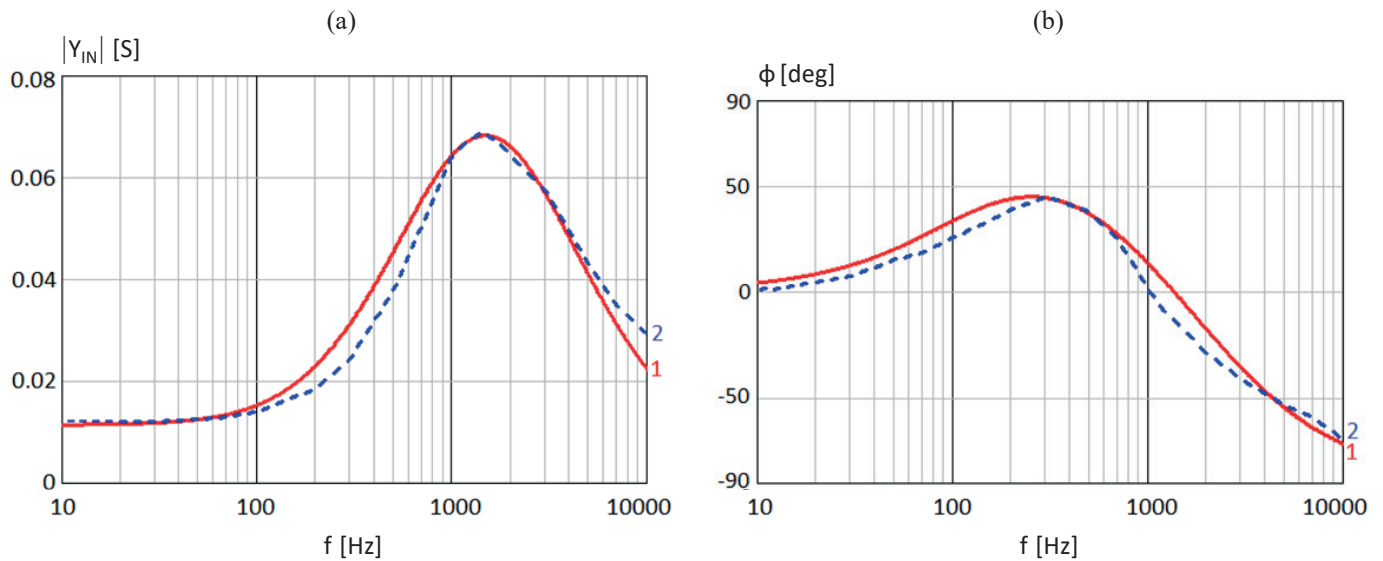


Fig. 12. Frequency dependence of the input admittance Y_{in} obtained from the small-signal model (1) or from the full-wave Spice simulations (2) for CCM ($R_L = 3 \Omega$): a) magnitude; b) phase

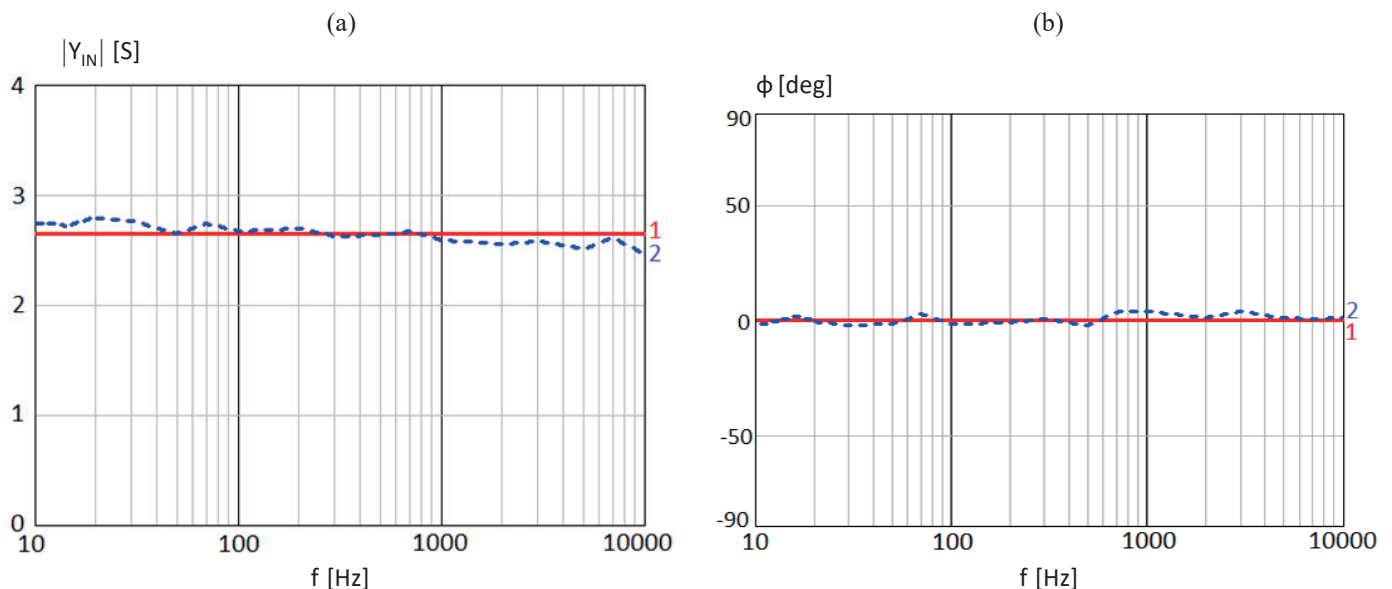


Fig. 13. Frequency dependence of the input admittance Y_{in} obtained from the small-signal model (1) or from the full-wave Spice simulations (2) for DCM ($R_L = 50 \Omega$): a) magnitude; b) phase

5. Conclusions

The analysis, simulations and measurements of the input characteristics of a non-ideal flyback DC-DC converter are presented in the paper. The DC and AC characteristics are considered with the special attention paid to the differences in the features of the converter in continuous conduction and discontinuous conduction modes (CCM and DCM). The calculations based on formulas derived in the paper are compared with the results of full-wave Spice simulations and measurements performed in the laboratory model of flyback converter and relatively good consistency has been obtained. The influence of parasitic effects

in the converter resulting from series resistances of transformer windings, output capacitor and semiconductor switches, leakage inductances of transformer and capacitances of switches on converter input characteristics has been observed. The results of this work can be helpful in the design of power systems based on flyback converters, especially AC-DC converters with power factor correction (PFC).

REFERENCES

- [1] R.W. Erickson and D. Maksimovic, “*Fundamentals of Power Electronics*”, 2-nd Edition, Kluwer, 2002.

- [2] M.K. Kazimierczuk, "Pulse-Width Modulated DC-DC Power Converters", J. Wiley, 2008.
- [3] D.W. Hart, "Power Electronics", McGraw-Hill, New York, 2011.
- [4] W. Janke, "Averaged Models of Pulse-Modulated DC-DC Converters", Part II. Models Based on the Separation of Variables, *Archives of Electrical Engineering* 61(4), 633–654 (2012).
- [5] W. Janke, "Equivalent Circuits for Averaged Description of DC-DC Switch-Mode Power Converters Based on Separation of Variables Approach", *Bull. Pol. Ac.: Tech.* 61(3), 711–723 (2013).
- [6] T.T. Vu, S. O'Driscoll, and J.V. Ringwood, "Primary-side sensing for a flyback converter in both continuous and discontinuous conduction mode", *ISSC 2012*, NUI Maynooth, June 28–29.
- [7] T.T. Vu, *Non-linear Dynamic Transformer Modelling and Optimum Control Design of Switched-mode Power Supplies*, PhD Thesis, National University of Ireland Maynooth, 2014.
- [8] S.Y. Chen, "Small-Signal Model for a Flyback Converter with Peak Current Mode Control", *IET Power Electronics* 7(4), 805–810, Apr. 2014.
- [9] S. Xu, X. Zhang, C. Wang, and W. Sun, "High Precision Constant Voltage Digital Control Scheme for Primary-Side Controlled Flyback Converter", *IET Power Electronics* 9(13), 2522–2533 (2016).
- [10] A. Ayachit, A. Reatti, and M.K. Kazimierczuk, "Magnetising inductance of multiple-output flyback dc-dc convertor for discontinuous-conduction mode", *IET Power Electronics* 10(4), 451–461 (2017).
- [11] C.H. Cheng, C.J. Chen, and S.S. Wang, Small-Signal Model of Flyback Converter in Continuous-Conduction Mode with Peak-Current Control at Variable Switching Frequency, *IEEE Trans. on Power Electronics* 33(5), 4125–4156, May 2018.
- [12] K. Soltanzadeh and R. Yousefi, "Analysis and design of two-switch flyback converter with double passive lossless snubber", *IET Power Electronics* 11(7), 1187–1194 (2018).
- [13] S.A. Akbarabadi, H. Atighechi, and J. Jatskevich, "Circuit-Averaged and State-Space-Averaged-Value Modeling of Second-Order Flyback Converter in CCM and DCM Including Conduction Losses", *4th International Conference on Power Engineering, Energy and Electrical Drivers*, pp. 995–1000, Istanbul, Turkey, 13–17 May 2013.
- [14] A.A. Saliva, "Design Guide for Off-line Fixed Frequency DCM Flyback Converter", Infineon, Design Note DN 2013–01, V1.0 January 2013.
- [15] M. Ivankovic, "CrCM Flyback PFC Converter Design", Infineon, Design Note DN 2013–11, V1.0 January 2013.
- [16] C. Larouci, A. Chaibet, T. Azib, and M. Boukhnifer, "Control of a Flyback Converter in Mixed Conduction Mode: Influence on the Converter Design Using Optimization under Constraints", *IEEJ Journal of Industry Applications* 2(3), 132–140 2013.
- [17] P.C.-P. Chao, W.-D. Chen, and R.-H. Wu, "A battery charge controller realized by a flyback converter with digital primary side regulation for mobile phones", *Microsystem Technologies* 20, 1689–1703, 2014.
- [18] H.-C. Lin, W.-M. Chu, C.-H. Tsai, and W.-C. Su, "A digitally variable on-time controlled PFC flyback converter with primary-side regulation", *7th International Symposium on Next Generation Electronics (ISNE 2108)*, ISSN: 2378–8607.
- [19] J. Sun, D. Mitchell, M. Greuel, P. Krein, and R. Bass, "Averaged modeling of PWM Converters Operating in Discontinuous Conduction Mode", *IEEE Trans. on Power Electronics* 16(4), 482–492 (2001).
- [20] W. Janke, M. Bączek, and J. Kraśniewski, "Large signal averaged models of the non-ideal flyback converter derived by the separation of variables", (to be published).
- [21] R. Ridley, "Flyback Converter – Snubber Design", *Switching Power Magazine – Designers Series XII*, 2005.